

Modelling and classification of tubular joint rigidity and its effect on the global response of CHS lattice girders

Wei Wang[†] and Yiyi Chen[‡]

College of Civil Engineering, Tongji University, Shanghai 200092, China

(Received January 28, 2005, Accepted September 7, 2005)

Abstract. In engineering practice, tubular connections are usually assumed pinned or rigid. Recent research showed that tubular joints may exhibit non-rigid behavior under axial or bending loads. This paper is concerned with establishing a new classification for tubular joints and investigating the effect of joint rigidity on the global behavior of CHS (Circular Hollow Section) lattice girders. Parametric formulae for predicting tubular joint rigidities are proposed, which are based on the finite element analyses through systematic variation of the main geometric parameters. Comparison with test results proves the reliability of these formulae. By considering the deformation patterns of respective parts of Vierendeel lattice girders, the boundary between rigid and semirigid tubular connections is built in terms of joint bending rigidity. In order to include characteristics of joint rigidity in the global structural analysis, a type of semirigid element which can effectively reflect the interaction of two braces in K joints is introduced and validated. The numerical example of a Warren lattice girder with different joint models shows the great effect of tubular joint rigidities on the internal forces, deformation and secondary stresses.

Key words: non-rigid behavior; tubular joint rigidity; finite element analysis; tubular joints classification; semirigid element; CHS lattice girder.

1. Introduction

Since the beginning of their commercial use four decades ago, steel tubular structures have been increasingly popular, especially in large open areas with few or no intermediate supports. Over the years, they have become known for their pleasing appearance, light weight, easy fabrication and rapid erection. Hundreds of successful tubular truss applications now exist all over the world covering stadiums, public halls, exhibition centers, aeroplane hangers and many other buildings.

The majority of steel tube structures employ tubular connections. Existing research focused on ultimate capacity of tubular connections under axial brace loads as their main target. However, the loaded braces always cause local distortion of the chord cross-section and hence displacements and rotations of the ends of the braces relative to the chord axes. Non-rigid behavior of this joint will redistribute the nominal stresses, increase the deflections, influence the critical buckling loads and natural frequencies.

In recent years, some research results on rigidity or static strength of tubular joints under bending

[†] Ph.D., Corresponding author, E-mail: weiwang@mail.tongji.edu.cn

[‡] Professor

loads or combined axial and bending loads have been reported by several researchers, including experimental investigations on CHS T connections under combined bending and axial loads on the braces (Kurobane 1991) and numerical investigations on CHS X, T, Y and K connections (Vegte 1995, Lee 1994, Healy 1993, Healy 1994, Gazzola 2001) and on RHS T and X connections (Yu 1997). The formulae for the ultimate bending capacity of tubular joints have been recommended in CIDECT design guide (Wardenier *et al.* 1991). It also noted that the bending rigidities of tubular joints may have great effect on the moment distribution of static indeterminate structural systems. Choo (2004) carried out a parametric numerical study on the static strength of doubler and collar plate reinforced X joints loaded by in-plane bending and provided design recommendations for this joint type. Fessler (1986) tested 25 Araldite model tubular joints, including seven multi-brace joints and derived parametric equations for the flexibility matrices of single brace joints. This was the only published previous work in which the cross-flexibilities between two braces at a point had been measured. Ure (1993) presented a method of determining local joint flexibility of flattened-ended tubular connections using finite element modeling. Hyde (1998) and Leen (2000) adopted an energy-based approach to predict elastic-plastic displacement of tubular joints under combined loading. Furukawa (1998) proposed effective column length of web members in CHS lattice girder based on the study on out-of-plane rotational stiffness of CHS joints. France (1999) carried out experimental research on the strength and rotational stiffness of simple connections to tubular columns using flowdrill connectors.

Since real tubular connections possess some stiffness, which falls between the two extreme cases of fully rigid and ideally pinned, the modeling of connections as semirigid is more realistic. However, in engineering practice some connections can be considered pinned while some connections can be considered rigid. For example, the conventional procedure for the design and analysis of offshore structures is to assume that the joints are completely rigid. On the other side, in the tubular trusses for buildings, the members are usually supposed as pin-connected. But when eccentricities exceed a certain range between $-0.55D$ and $0.25D$, it is common practice to use continuous chords with the braces connected with pins to the chord. The assumption of ideally pinned or rigid connections considerably simplifies the design and analysis procedures. Therefore, it is important to estimate in advance whether the connections can be assumed rigid, semirigid, or pinned.

Proposals for the clear classification of beam-to-column connections have been presented by BJORHovde (1990), EN1993-1-1 (2005), Goto (1998), Nethercot (1998) and Hasan (1998). In addition, EN1993-1-8 proposes the following design recommendation of steel tube lattice girder with diagonal braces for building structures: secondary moments at the joints, caused by the rotational stiffness of the joints, may be neglected provided that the ratio of the system length to the members depth in the plane of the girder is not less than 6. But for Vierendeel lattice girders and tubular framed structures, there is no available joint classification to apply.

A natural extension of work on the determination of joint rigidity is the incorporation of these rigidities in a typical structure so that their influence on internal force (and hence stress) distribution, overall displacement can be evaluated. For fulfilling this goal, it is necessary to establish a reasonable model to reflect the characteristic of tubular joints and involved it into existing or developed computer programs. Generally, there are three types of method in numerical modelling of steel tube structures (Kurobane 1998). The most accurate method is to model tubular connections as three-dimensional finite element substructures. In this way, the influence of the geometry of the connections is directly taken into account. Even the governing extrapolated

geometric stresses at the weld toes can be determined directly. However, this method requires sufficient computer capacity. Only specialized researchers, who are familiar with the use of correct elements and meshes, can handle this method at present. Another method is to model the chords with continuous beams and the braces are connected by springs representing the connection rigidity to the chord. Eccentricities should be incorporated in the model. In this way the proper bending moments in the members can be determined. But for K tubular joints, the interaction between two braces cannot be reflected by this method. The third method is that an effective length is adopted to replace the real length of the brace, so that the leading diagonal elements of the stiffness matrix of the members can be modified. However, this method is an approximate one. Only when lacking the rigidity characteristics of joints is this simplification used.

In the first portion of this paper, tubular joint rigidity is defined based on their local deformation behavior. The finite element analyses are adopted to carry out an extensive parametric study on the rigidity of CHS T, Y and K joints loaded by axial force and in-plane bending. In the parametric study, the effects of the main geometric parameters on the axial and bending rigidity of the joints are investigated respectively. Based on the discussion of the mechanism of these effects, mathematical models of parametric formulae are introduced. By using orthogonal design method and multi-variable nonlinear regression analysis, parametric formulae for rigidities of CHS joints are established. These results are then verified against available experimental results by authors and from Makino test database. In the second portion of this paper, a new classification for tubular joints in Vierendeel lattice girders is proposed in terms of the boundary between rigid and semirigid connections. Furthermore, it is compared with the classification for beam-to-column connections proposed by EC3. In order to include parametric formulae for CHS joint rigidity in the global structural analysis, a numerical methodology which involves semirigid elements to connect braces to chords is introduced in the third portion. The corresponding computer program of global analysis of CHS lattice girders is compiled. A Warren lattice girder is chosen as a numerical example for illustration. The internal forces, overall deformation and secondary stresses of members are computed with different joint models and compared with that by conventional rigid or pinned joint assumptions.

2. Modeling of tubular connections

2.1 Definition and determination of tubular joint rigidity

When braces are subjected to axial loads, axial displacement occurs at the ends of the braces relative to the chord axes. When braces are subjected to bending moments, there also occurs rotations of the ends of the braces relative to the chord axes. Based on this deformation behavior, tubular joint rigidity is defined as the force causing unit deformation.

For T and Y tubular joints, the following definitions are applied

$$K_N = \frac{P}{\delta}, \quad K_M = \frac{M}{\theta_r} \quad (1)$$

where K denotes the rigidity of tubular joints. Subscripts N and M denote the loading cases of axial force and in-plane bending respectively. δ is the local translational displacement at the intersection between the brace and the chord wall, which is caused by the axial force P and is in the direction of

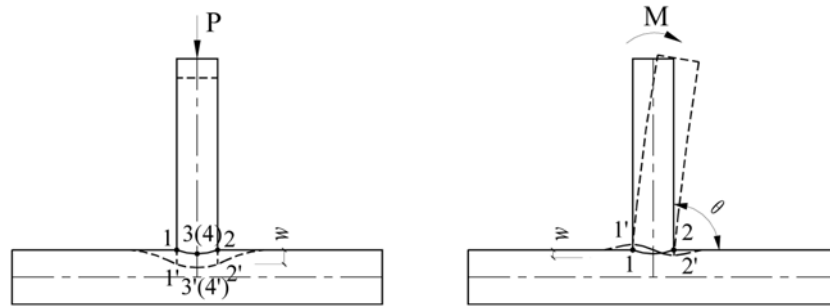


Fig. 1 Local deformation of T tubular joint

brace axis. θ_r is the local in-plane rotation at the same point, which is caused by the in-plane bending moment M .

In practical calculation, crown points and saddle points of a tubular joint are chosen as reference locations to determine δ and θ_r . As shown in Fig. 1, the deformation at point 1, 2, 3 and 4, denoted as w_1 , w_2 , w_3 and w_4 , is the local wall convex or concave normal to chord axis in the plane of chord and brace axis, exclusive of the global deflection of the chord as a beam. Thus the total axial displacement δ and the in-plane rotation θ_r is computed as follows:

$$\delta = \frac{w_1 + w_2 + w_3 + w_4}{4} \sin \theta \quad (2)$$

$$\theta_r = \frac{w_1 - w_2}{d - t} \sin \theta \quad (3)$$

So the joint rigidity is determined from the following equations,

$$K_N = (4P) / [(w_1 + w_2 + w_3 + w_4)(\sin \theta)] \quad (4)$$

$$K_M = M(d - t) / [(w_1 - w_2) \sin \theta] \quad (5)$$

where θ is the initial angle between the brace and the chord, d and t are the brace diameter and thickness respectively.

For K tubular joints, a joint rigidity matrix must be defined as follows since axial forces and in-plane bending interact and deformation of one brace cause deformations of the other brace in the same joint:

$$\{P_1, M_1, P_2, M_2\}^T = [K]_L \{\delta_1, \theta_{r1}, \delta_2, \theta_{r2}\}^T \quad (6)$$

where $[K]_L$ is the joint rigidity matrix and can be formulated as

$$[K]_L = \begin{bmatrix} k_{11} & k_{12} & k_{13} & k_{14} \\ k_{21} & k_{22} & k_{23} & k_{24} \\ k_{31} & k_{32} & k_{33} & k_{34} \\ k_{41} & k_{42} & k_{43} & k_{44} \end{bmatrix} \quad (7)$$

The leading diagonal terms of $[K]_L$ represent the relation between forces and corresponding displacements or rotations. The terms off the leading diagonal represent the interaction between two braces. Due to the reciprocal theorem, this matrix is symmetric, therefore

$$k_{12} = k_{21}, \quad k_{13} = k_{31}, \quad k_{14} = k_{41}, \quad k_{23} = k_{32}, \quad k_{24} = k_{42}, \quad k_{34} = k_{43} \quad (8)$$

For the convenience of finite element calculation, Eq. (6) is expressed equivalently as

$$\{\delta_1, \theta_{r1}, \delta_2, \theta_{r2}\}^T = [f]_L \{P_1, M_1, P_2, M_2\}^T \quad (9)$$

where $[f]_L$ is the joint flexibility matrix and can be formulated as

$$[f]_L = \begin{bmatrix} f_{11} & f_{12} & f_{13} & f_{14} \\ f_{21} & f_{22} & f_{23} & f_{24} \\ f_{31} & f_{32} & f_{33} & f_{34} \\ f_{41} & f_{42} & f_{43} & f_{44} \end{bmatrix} \quad (10)$$

2.2 FE modeling and analysis

The finite element method is used to perform the analyses contained in this study. All analyses are accomplished using the general purpose FE package program ANSYS (2002).

2.2.1 Geometry configuration

Fig. 2 shows the configuration of CHS joints and definitions of main geometric parameters. In the finite element study, the length-to-radius ratio of the chord, $\alpha = 2L/D = 20$, and the brace length is kept greater than three times the brace diameter ($l_i > 3d_i, i = 1, 2$). The symmetry of the geometry and loading conditions is used so that only a semi-tubular part is modelled. A rigid cap is added at each brace tip to avoid the local distortion which probably influence the stress distribution and deformation in joint zone. In analyses, explicit modeling of the weld fillets is omitted. It has been found through experience that such modeling usually had a negligible effect on the rigidity of tubular joints (Dexter *et al.* 1996).

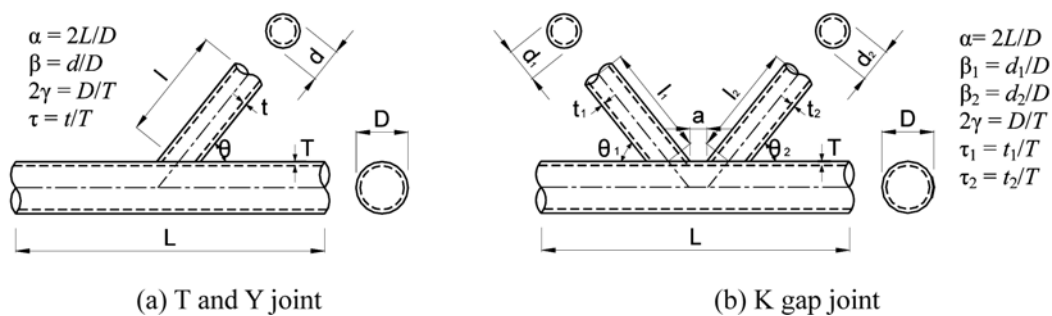


Fig. 2 Joint description and parameter definitions

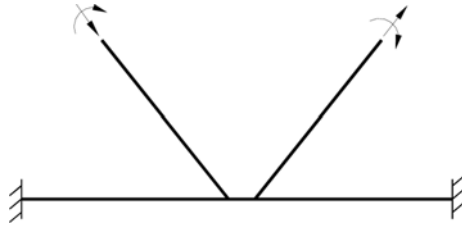


Fig. 3 Boundary conditions for chord and brace ends

2.2.2 Load application method

For joints loaded by in-plane bending, in order to simplify the analysis the existence of transverse shear force is excluded, so a concentrated moment causing the brace to rotate in the direction of the acute brace angle is applied to the brace end plate. For axially loaded joints, uniformly distributed pressure is applied to the rigid cap at the brace tip.

2.2.3 Element type and material properties

8-Node structural shell element (ANSYS element type SHELL93) is used in the FE models. It is particularly well suited to model curved shells. The element has six degrees of freedom at each node: translations in the nodal x , y , and z directions and rotations about the nodal x , y , and z -axes. The deformation shapes are quadratic in both in-plane directions. The element and node numbers of the FE models are around 3000 and 6500 respectively.

The steel material is isotropic with an elastic modulus E of 206000 MPa and Poisson's ratio of 0.3.

2.2.4 Boundary conditions

The chord and brace boundary conditions applied to the models are shown in Fig. 3. The fixed conditions are applied to the nodes of both chord ends. Since the brace and chord lengths are chosen to avoid end effects, the boundary conditions should not influence the joint rigidity. In addition, symmetry boundary conditions are applied along the plane of symmetry.

2.3 Influence of geometric parameters on tubular joint rigidity

Fig. 4 and Fig. 6 present plots of nondimensional rigidity by FE analysis against β , γ , τ and $\sin\theta$, respectively. Fig. 5 and Fig. 7 show joint rigidity by FE analysis against chord diameter D . Also plotted is a curve corresponding to the mean calculated by a regression analysis. As can be seen, when chord diameter D is kept constant, axial or bending rigidity of a tubular joint decrease as γ , τ or $\sin\theta$ increases, and as β decreases. The parameters which most influences joint rigidity are β and γ . Joint rigidity is almost identical for the parameter τ between 0.2 and 0.8. This means τ has little influence on the joint rigidity. Therefore, in the regression analysis to obtain the rigidity formulae for K joints in section 2.5, the function of τ is omitted.

For a proper understanding of the behavior of tubular joints it is important to consider the mechanism of load transfer.

A mechanical model which represents the behavior of joints can be simplified as follows:

For joints loaded by in-plane bending, bending moment can be represented by a couple of forces which act perpendicular to the chord axis at a distance of brace diameter d from each other along

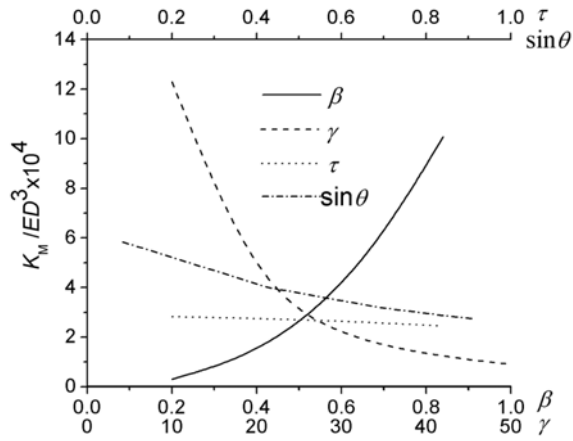


Fig. 4 Effect of geometric parameters on bending rigidity

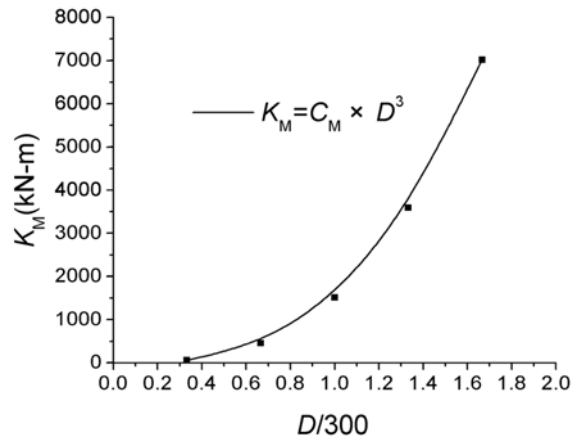


Fig. 5 Effect of chord diameter on bending rigidity

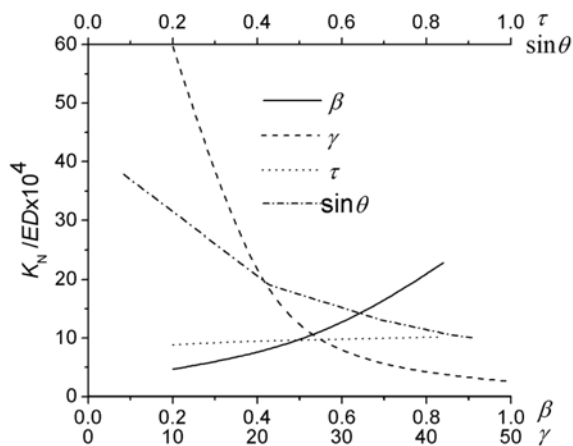


Fig. 6 Effect of geometric parameters on axial rigidity

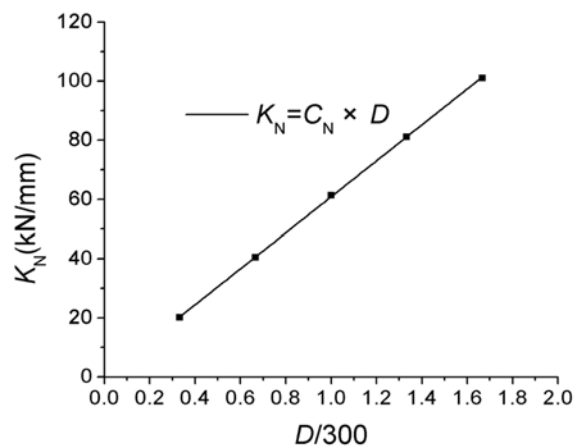


Fig. 7 Effect of chord diameter on axial rigidity

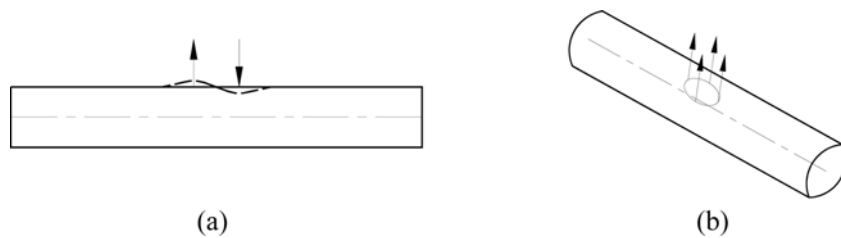


Fig. 8 Simplified mechanical model of tubular joint

the chord axis (Fig. 8a). For axially loaded joints, brace load can be replaced by four concentrated forces acting in the saddle points and crown points at the intersection of the chord and brace respectively (Fig. 8b).

The load has to be transmitted to the chord by bending. Thus, the local deformation is determined by the bending stiffness of the top face of the chord section. Bending stiffness of unit width shell can be expressed in Eq. (11).

$$D_s = \frac{Et_s^3}{12(1-\nu^2)} \quad (11)$$

where t_s is the thickness of the shell, ν is the Poisson's ratio, E is the modulus of elasticity.

For joints under bending, as β increases, the distance between the couple of forces, d , increases. When M is kept constant, the force value decreases. The local vertical deformations of crown points therefore reduce, with joint bending rigidity increased. By definition, γ increases as t_s decreases and hence in Eq. (11), D_s decreases. As $\sin\theta$ increases, the area of the intersection is smaller, leading to the reduction in overall bending stiffness of the chord top face. Both cases cause the decrease of joint bending rigidity. The axial rigidity of tubular joints vary in a similar manner.

By single parameter analysis, the following mathematic expressions for axial rigidity, K_N , and bending rigidity, K_M , of tubular joints could take the form:

$$K_N = C_N \cdot ED \cdot Q_g \quad (12)$$

$$K_M = C_M \cdot ED^3 \cdot Q_g \quad (13)$$

where, C_N and C_M are multipliers, Q_g is a geometric function, i.e., $Q_g = f(\theta, \beta, \gamma, \tau)$.

2.4 Joint models setup

A method for choice of experimental parameters called orthogonal design method is adopted to cover all possible configurations of tubular joints. For T and Y joints, each of the four parameters is varied in three level values to create a total of 9 joint models. For K joints, each of the six parameters is varied in five level values to create a total of 25 joint models. The main geometric parameters involved in this study are summarized in Tables 1 and 2, which are chosen to cover the practical range of joint configurations found in steel tube structures.

Table 1 Parametric value of T & Y joint

level	β	γ	τ	θ
1	0.20	10	0.2	30°
2	0.55	30	0.6	60°
3	0.90	50	1.0	90°

Table 2 Parametric value of K joint

level	γ	β_1	β_2	θ_1	θ_2	a/D
1	10	0.1	0.1	30°	30°	0.01
2	20	0.3	0.3	45°	45°	0.25
3	30	0.5	0.5	60°	60°	0.50
4	40	0.7	0.7	75°	75°	0.75
5	50	0.9	0.9	90°	90°	1.00

2.5 Parametric formulae

Statistical analysis tools are used for the non-linear regression of finite element results. The following function types are considered in the regression phase of this study: linear models, exponential, logarithm, polynomial, and trigonometric functions.

Equations based on power and exponential functions are successfully fitted to all data in terms of β , γ , τ and θ . Almost all individual data points are within 10% of calculated values. The following parametric formulae for predicting joint rigidities show the results of multiple regression analysis:

For T and Y joints,

$$K_N = 0.105ED(\sin\theta)^{-2.36}\gamma^{-1.90}\tau^{-0.12}e^{2.44\beta} \quad (14)$$

$$K_M = 0.362ED^3(\sin\theta)^{-1.47}\gamma^{-1.79}\tau^{-0.08}\beta^{2.29} \quad (15)$$

where, $30^\circ \leq \theta \leq 90^\circ$, $0.2 \leq \beta \leq 1.0$, $10 \leq \gamma \leq 50$, $0.2 \leq \tau \leq 1.0$.

For K joints,

$$f_{11} = \frac{1}{ED}(\sin\theta_1)^{2.11}(\sin\theta_2)^{0.12}\gamma^{1.86}\beta_1^{-0.78}\beta_2^{-0.06}e^{0.34a/D} \quad (16)$$

$$f_{12} = f_{21} = f_{34} = f_{43} = 0 \quad (17)$$

$$f_{13} = f_{31} = \frac{0.904}{ED}(\sin\theta_1)^{0.95}(\sin\theta_2)^{1.19}\gamma^{1.80}\beta_1^{-0.38}\beta_2^{-0.45}e^{-0.13a/D} \quad (18)$$

$$f_{14} = f_{41} = \frac{0.556}{ED^2}(\sin\theta_1)^{0.56}(\sin\theta_2)^{-0.08}\gamma^{1.63}\beta_1^{-0.82}\beta_2^{-0.27}e^{-0.11a/D} \quad (19)$$

$$f_{22} = \frac{2.994}{ED^3}(\sin\theta_1)^{1.19}(\sin\theta_2)^{0.12}\gamma^{1.72}\beta_1^{-2.19}\beta_2^{0.02}e^{0.14a/D} \quad (20)$$

$$f_{23} = f_{32} = \frac{0.556}{ED^2}(\sin\theta_1)^{-0.08}(\sin\theta_2)^{0.56}\gamma^{1.63}\beta_1^{-0.27}\beta_2^{-0.82}e^{-0.11a/D} \quad (21)$$

$$f_{24} = f_{42} = \frac{2.088}{ED^3}(\sin\theta_1)^{-0.22}(\sin\theta_2)^{0.12}\gamma^{1.26}\beta_1^{-0.53}\beta_2^{-0.67}e^{-0.94a/D} \quad (22)$$

$$f_{33} = \frac{1}{ED}(\sin\theta_1)^{0.12}(\sin\theta_2)^{2.11}\gamma^{1.86}\beta_1^{-0.06}\beta_2^{-0.78}e^{0.34a/D} \quad (23)$$

$$f_{44} = \frac{2.994}{ED^3}(\sin\theta_1)^{0.12}(\sin\theta_2)^{1.19}\gamma^{1.72}\beta_1^{0.02}\beta_2^{-2.19}e^{0.14a/D} \quad (24)$$

where, f_{ij} are the terms in the joint flexibility matrix in Eq. (10) and $30^\circ \leq \theta_1, \theta_2 \leq 90^\circ$, $0.2 \leq \beta_1, \beta_2 \leq 1.0$, $10 \leq \gamma \leq 50$, $0 \leq a/D \leq 1.0$.

2.6 Comparison with test results

The available test results for comparison with the parametric formulae in this paper came from the Makino database (Makino *et al.* 1996) which contains data relating to full-scale failure tests on T tubular joints and a number of loading tests on CHS tubular joints carried out by the authors at Tongji University (Chen and Wang 2003).

Tables 3 and 4 summarize the results of the comparison between the estimated rigidities using the authors' formulae and the test results from Makino database. Overall, the formulae above show good agreement with experimental results. TC-14 and TC-17 have nearly identical geometric parameters but the test results are different, this may be due to variability in the test.

Table 3 Test results compared with the authors' formulae for bending rigidity

Specimen	β	γ	τ	θ	K_M (test) (kN-m)	K_{Mj} (Eq.) (kN-m)	K_M/K_{Mj}
TM-33	0.36	14.6	0.97	90°	279	284	0.98
TM-35	1.00	14.8	1.0	90°	2680	2852	0.94
TM-36	0.36	24.4	1.0	90°	115	112	1.02
TM-38	1.00	23.8	1.0	90°	1430	1234	1.16

Table 4 Test results compared with the authors' formulae for axial rigidity

Specimen	β	γ	τ	θ	K_N (test) (kN/mm)	K_{Nj} (Eq.) (kN/mm)	K_N/K_{Nj}
TC-12	0.44	35.4	0.98	90°	24.5	23.0	1.07
TC-13	0.20	46.7	0.61	90°	12.7	11.4	1.11
TC-14	0.36	46.7	0.96	90°	19.6	16.2	1.21
TC-17	0.36	46.9	0.97	90°	16.7	16.0	1.04
TC-115	1.00	23.8	1.00	90°	86.1	101.0	0.85

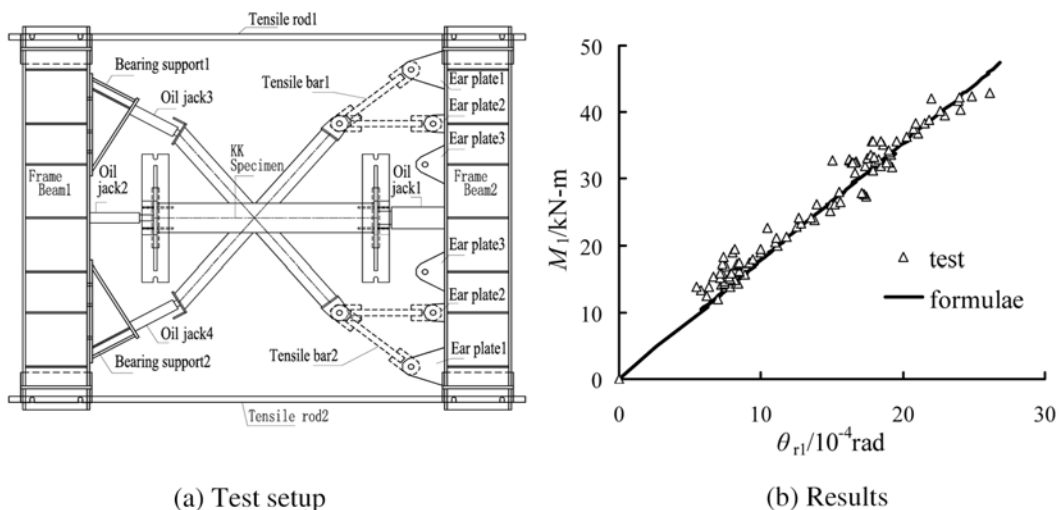


Fig. 9 Comparison of parametric formulae with test value for K tubular joint

In addition, an experimental research on the rigidity of uni-planar KK tubular joint (Fig. 9a) was performed at Tongji University (Chen and Wang 2003). It can be expected that the braces on the other side of the chord have almost no effect on one side in elastic range, so the test results can be used to judge the validity of the parametric formulae for K joints. According to Eqs. (9) and (10), the evaluation of the rigidity of a K joint definitely relates to the local axial deformation and the interaction between the two braces. Comparison of the authors' parametric formulae for K joints with test values is made graphically in Fig. 9(b), which plots M_1 against θ_{r1} as described in Eq. (9). The parametric formulae provide a good fit to the test results. It can be concluded that the formulae proposed in this paper are reliable on the whole in evaluating the local rigidity of tubular joints and can be recommended for use in the global structural analysis of steel-tube structures.

3. Classification by rigidity of tubular joints in Vierendeel lattice girders

A Vierendeel lattice girder is a type of girder without diagonals in which shear forces are resisted by the vertical braces and chords, acting together as moment-resisting frames. It may have diagonals in some bays in some designs, but may also be designed to rely totally on the verticals. The EC3 rules for joint classification are applicable to building frames (i.e., beams and columns) and not designed for lattice girders. So in this section, a classification for tubular joints in Vierendeel lattice girders is proposed in terms of the boundary between rigid and semirigid connections. The semirigid connection is represented by a rotational spring.

3.1 Subassemblage frame models

To take into account the behavior of lattice girders in the classification of connections, several subassemblages that will approximately represent the behavior of the respective parts of the

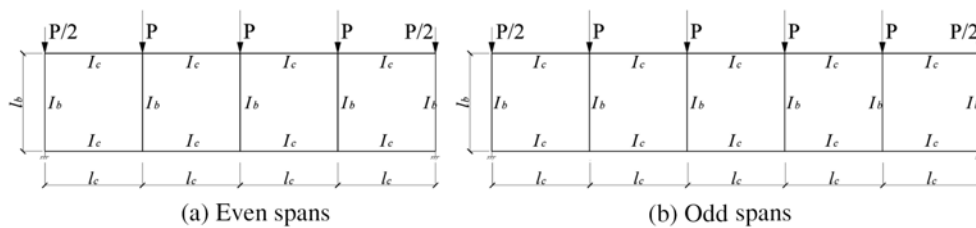


Fig. 10 Multispan Vierendeel lattice girders

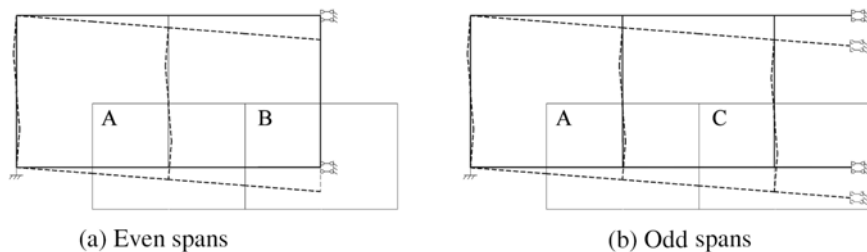


Fig. 11 Deformation pattern of Vierendeel lattice girders

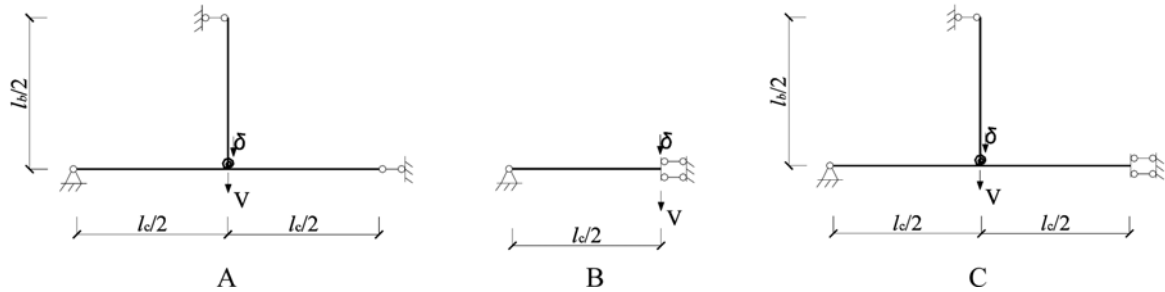


Fig. 12 Subassemblages

multispan lattice girders are adopted in Fig. 11. These subassemblages are chosen by considering the deformation patterns of the respective parts of the girders with odd or even spans illustrated in Fig. 10. The subassemblages so chosen are summarized in Fig. 12. In this figure, the notations A~C denote how the respective subassemblages represent the parts of the girders in Fig. 11.

3.2 Classification criteria

Joint bending rigidities have a large influence on the behavior of lattice girders at the serviceability limit state. Thus, the following criteria defined in terms of displacements is used to classify the semirigid connections as rigid

$$\Delta = (\delta_s - \delta_r) / \delta_r \quad (25)$$

where δ_s = displacement of a lattice girder with semirigid connections; and δ_r = displacement of the corresponding rigid lattice girder.

The loading conditions used to calculate the displacements are shown in Fig. 12. In the following, the boundary value of the joint bending rigidity between rigid and semirigid connections will be derived by considering the behavior of the lattice girders with odd or even spans.

3.3 Derivation of boundary between rigid and semirigid tubular connections

The boundary between rigid and semirigid connections is determined from Eq. (25) in terms of the joint bending rigidity. The displacements, δ_s and δ_r , in (25) are represented by the vertical displacements at the joint when a vertical force V is applied to the subassemblages, as shown in Fig. 12. In the calculation of δ_s and δ_r , the small displacement theory is applied because the displacements at the serviceability limit state are small. Furthermore, the rigidity of semirigid connections is assumed linearly elastic.

Here we show the procedure to derive the boundary between rigid and semirigid connections.

For the subassemblage A with a semirigid connection, the vertical displacement, δ_s , can be analytically obtained as

$$\delta_s = \frac{Vl_c^2}{12K_cK_b}(K_b + K_c) + \frac{Vl_c^2}{4K_M} = \frac{Vl_c^2}{12K_cK_bK_M}(K_MK_b + K_MK_c + 3K_cK_b) \quad (26)$$

where

$$K_b = \frac{EI_b}{l_b}, \quad K_c = \frac{EI_c}{l_c} \quad (27a,b)$$

Let $K_M \rightarrow \infty$, the vertical displacement of the subassembly A with a rigid connection is given by

$$\delta_r = \frac{Vl_c^2}{12K_cK_b}(K_b + K_c) \quad (28)$$

Substituting (26) and (28) into (25), the following condition is obtained:

$$\frac{K_M}{K_b} = \frac{3}{(1+G) \cdot \Delta} \quad (29)$$

where

$$G = \frac{K_b}{K_c} \quad (30)$$

If we adopt $G = 1.4$, which was assumed by EC3 to determine the boundary between rigid and semirigid beam-to-column connections, and $\Delta = 0.05$, K_M/K_b becomes 25. This value is equal to the boundary value which is given by EN1993-1-1 (2005).

For the subassembly B, the vertical displacement of the lattice girder has no correlation with joint bending rigidity, so the derivation of boundary for this case is neglected.

For the subassembly C with a semirigid connection, the vertical displacement, δ_s , can be analytically obtained as

$$\delta_s = \frac{Vl_c^2}{24K_c(3K_b + K_c)} \cdot (3K_b + 4K_c) + \frac{9Vl_c^2 \cdot K_b^2}{4K_M(3K_b + K_c)^2} = \delta_r + \frac{9Vl_c^2 \cdot K_b^2}{4K_M(3K_b + K_c)^2} \quad (31)$$

In the same way, the vertical displacement of the subassembly C with a rigid connection is given by

$$\delta_r = \frac{Vl_c^2}{24K_c(3K_b + K_c)} \cdot (3K_b + 4K_c) \quad (32)$$

Substituting (31) and (32) into (25), the following condition is obtained:

$$\begin{aligned} \frac{K_M}{K_b} &= \frac{54K_bK_c}{\Delta \cdot (3K_b + K_c)(3K_b + 4K_c)} \\ &= \frac{54G}{\Delta \cdot (3G + 1)(3G + 4)} \end{aligned} \quad (33)$$

If we adopt $G = 1.4$ and $\Delta = 0.05$, K_M/K_b becomes 35.5. This value is larger than 25, which is given by EC3 as the boundary value. Table 5 summarized the boundaries defined in terms of the joint bending rigidity. By comparison with boundary value in EC3, it can be found that the EC3 frame rules do not apply for the lattice girders because they didn't consider the deformation behavior in different parts of the structures.

Table 5 Boundary value K_M^b for joint bending rigidity

Subassemblages	K_M^b/K_b
A	$\frac{3}{(1 + G) \cdot \Delta}$
B	N/A
C	$\frac{54G}{\Delta \cdot (3G + 1)(3G + 4)}$

4. Global structural analysis of steel tube lattice girder considering joint rigidity

4.1 Semirigid element representing tubular joint rigidity

In order to include characteristics of CHS joint rigidity in the global structural analysis, a type of semirigid element connecting braces to chords (Hu *et al.* 1993) are introduced and modified to model tubular joints in steel tube lattice girder.

For Y tubular joints, the brace and the chord are considered to be connected through a semirigid line element (see Fig. 13). Node *i* is the intersection of the brace axis and chord wall, node *k* is the intersection of the brace axis and chord axis. For K tubular joints, the semirigid element is a triangle connecting points *i*, *j* and *k* (see Fig. 14), Node *i* and *j* are the intersections of brace axes and chord wall respectively. Node *k* is obtained by projecting the intersection point of two brace axes onto the chord axis.

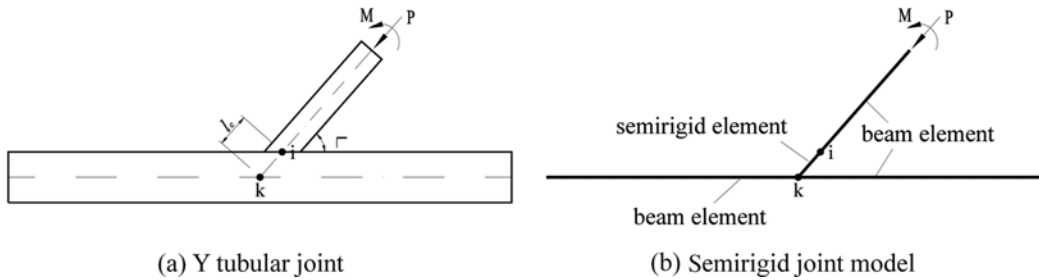


Fig. 13 Y tubular joint and its model in structural analysis

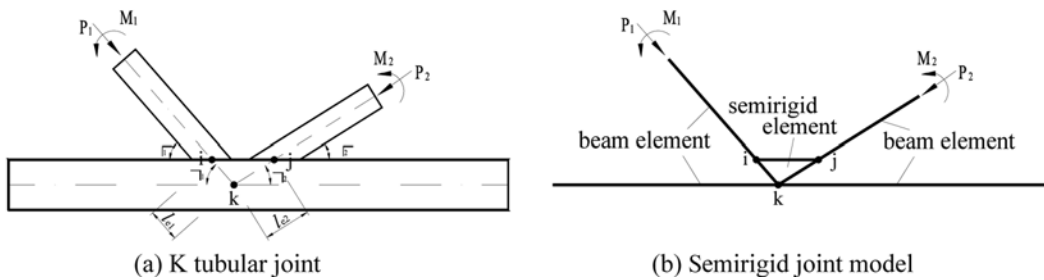


Fig. 14 K tubular joint and its model in structural analysis

By considering the relation between external loads acting on the tubular joint and local deformation of the joint, a stiffness matrix for the semirigid element is derived and can be expressed by the following equation.

$$[K] = [T][A]^{-1}[T]^T \quad (34)$$

For Y tubular joints,

$$[K] = \begin{bmatrix} K_{NX} & 0 & 0 & -K_{NX} & 0 & l_e \sin \theta K_{NX} \\ & K_{NY} & 0 & 0 & -K_{NY} & -l_e \cos \theta K_{NY} \\ & & K_M & 0 & 0 & -K_M \\ & & & K_{NX} & 0 & -l_e \sin \theta K_{NX} \\ \text{sym} & & & & K_{NY} & l_e \cos \theta K_{NY} \\ & & & & & l_e^2 \sin^2 \theta K_{NX} + l_e^2 \cos^2 \theta K_{NY} + K_M \end{bmatrix} \quad (35)$$

Since the stiffness of the chord wall in its axial direction is much greater than those in other directions, K_{NX} approaches infinity and

$$K_{NY} = K_N \sin^2 \theta \quad (36)$$

For K tubular joints, the matrices $[T]$ and $[A]$ in Eq. (34) are

$$[T] = \begin{bmatrix} 1 & 0 & 0 & 0 & 0 & 0 & -1 & 0 & l_{e1} \sin \alpha_1 \\ 0 & 1 & 0 & 0 & 0 & 0 & 0 & -1 & l_{e1} \cos \alpha_1 \\ 0 & 0 & 1 & 0 & 0 & 0 & 0 & 0 & -1 \\ 0 & 0 & 0 & 1 & 0 & 0 & -1 & 0 & l_{e2} \sin \alpha_2 \\ 0 & 0 & 0 & 0 & 1 & 0 & 0 & -1 & -l_{e2} \cos \alpha_2 \\ 0 & 0 & 0 & 0 & 0 & 1 & 0 & 0 & -1 \end{bmatrix}^T \quad (37)$$

$$[A] = \begin{bmatrix} \frac{1}{K_{NX1}} & 0 & 0 & 0 & 0 & 0 \\ 0 & \frac{f_{11}}{\sin^2 \theta_1} & 0 & 0 & \frac{f_{13}}{\sin \theta_1 \sin \theta_2} & \frac{-f_{14}}{\sin \theta_1} \\ 0 & 0 & f_{22} & 0 & \frac{f_{23}}{\sin \theta_2} & -f_{24} \\ 0 & 0 & 0 & \frac{1}{K_{NX2}} & 0 & 0 \\ 0 & \frac{f_{31}}{\sin \theta_1 \sin \theta_2} & \frac{f_{32}}{\sin \theta_2} & 0 & \frac{-f_{33}}{\sin^2 \theta_2} & 0 \\ 0 & \frac{-f_{41}}{\sin \theta_1} & -f_{42} & 0 & 0 & f_{44} \end{bmatrix} \quad (38)$$

Since axial tension and compression of the chord wall can be neglected, K_{NX1} and K_{NX2} approach infinity. After substituting parametric formulae in section 2.5 into Eqs. (35) and (38), the stiffness matrix of the semirigid element can be easily incorporated into a computer program developed by the authors to carry out the global structural analysis of steel tube lattice girders.

4.2 Validation of the methodology

In order to assess the capability of the present methodology to accurately represent the behavior of actual steel tube structures, a finite shell element model (Fig. 15) of a CHS lattice girder was created using the ANSYS software. The dimension of the tubes are: chord tube 168×12 (mm), brace tube 127×8 (mm). For comparison, the structure is analyzed with and without the present semirigid (Fig. 16) respectively.

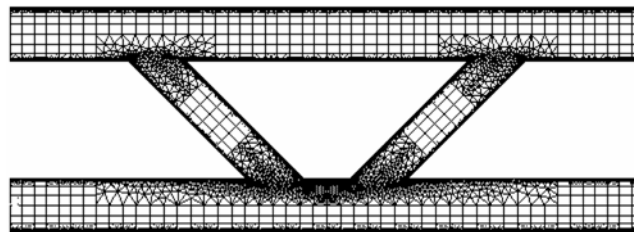


Fig. 15 Shell element model for a CHS lattice girder

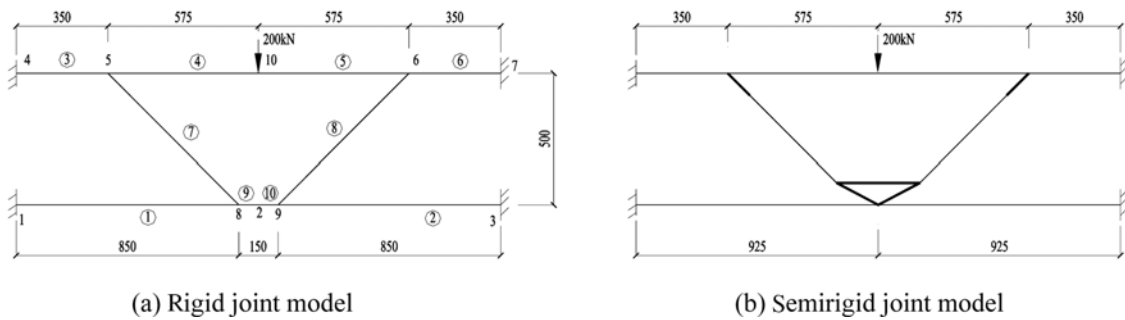


Fig. 16 Line element models for a CHS lattice girder

Table 6 Results of the numerical analysis for CHS lattice girder

		Node	δ_{semi}	δ_{rigid}	δ_{shell}	Element	Node	δ_{semi}	δ_{rigid}	δ_{shell}
Vertical deflection	Maximum normal stress	2	-0.44	-0.38	-0.46	1	1	-43.3	-46.9	-40.2
		5	-0.45	-0.39	-0.50	3	4	172.5	140.6	200.8
						3	5	41.8	26.1	35.2
		10	-1.50	-1.33	-1.53	4	5	-70.1	-75.3	-68.3
					4	10	-199.4	-175.3	-264.5	

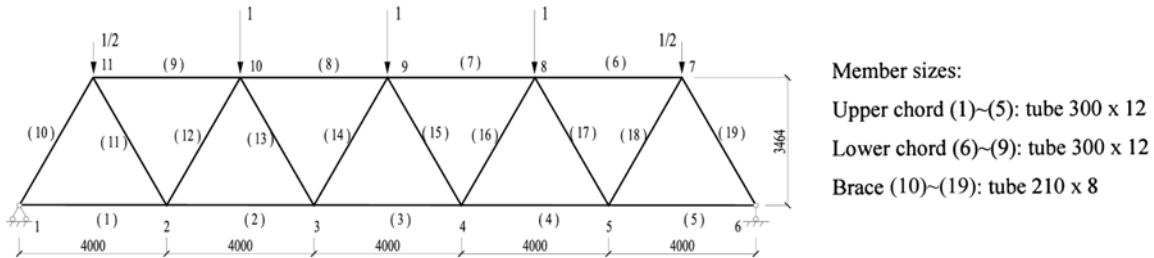


Fig. 17 Layout of lattice girder

The results of the validation study are presented in Table 6. The table shows that, when the semirigid element is included in the model, the predicted deflections and stresses are in better agreement with the results from shell finite element analysis than a rigid joint model.

The results of the validation study, presented in the tables above, indicate that the semirigid elements and the applied implementation methodology make the local joint rigidity of tubular joints under axial and in-plane bending loads represented effectively.

5. Warren lattice girder example

In order to investigate the effect of CHS joint rigidity on the local and overall response of Warren lattice girders, a typical simply supported truss shown in Fig. 17 is examined. Truss joints have a zero nodding eccentricity ($e = 0$) throughout. For this truss, six joint models are investigated in the analysis:

1. Model 1: all members including chords and braces are rigidly connected.
2. Model 2: all members including chords and braces are pin connected.
3. Model 3: chord-to-chord rigidly connected, while semirigid elements allowing for both joint axial and bending rigidity connect braces to chords, with interaction between two braces of K joints considered.
4. Model 4: the same as Model 3, except with no interaction between two braces of K joints considered.
5. Model 5: chord-to-chord rigidly connected, while semirigid elements allowing for only bending rigidity connect braces to chords, with joint axial rigidity treated as infinity.
6. Model 6: chord-to-chord rigidly connected, while semirigid elements allowing for only axial rigidity connect braces to chords, with joint bending rigidity treated as infinity.

Boundary conditions and unit loading of the truss are shown in Fig. 17. The results of the responses in the members from each of the models are compared in the following sections.

5.1 Effect of joint rigidity on axial forces

Table 7 lists axial force distribution in the members for each model of analysis. It can be seen from these analytical results that:

- for brace members closer to supports, their axial forces are larger. On the contrary, for chord members closer to supports, their axial forces are smaller.

Table 7 Axial forces of CHS lattice girder for different joint models

Member		Axial force (kN)					
		Model 1	Model 2	Model 3	Model 4	Model 5	Model 6
Lower chord	1	1.155	1.155	1.157	1.159	1.153	1.162
	2	2.865	2.887	2.861	2.857	2.867	2.857
	3	3.444	3.464	3.443	3.437	3.445	3.439
Upper chord	8	-3.155	-3.175	-3.155	-3.148	-3.156	-3.149
	9	-2.008	-2.021	-2.009	-2.005	-2.009	-2.007
Brace	10	-2.296	-2.309	-2.288	-2.290	-2.299	-2.285
	11	1.692	1.732	1.667	1.668	1.702	1.651
	12	-1.701	-1.732	-1.675	-1.680	-1.707	-1.663

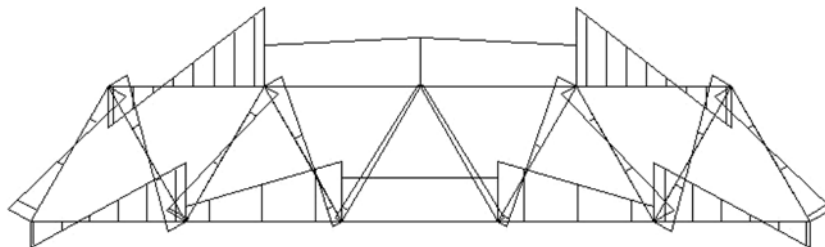
— the effect of joint rigidity on axial force in the chord is very small, the different theoretical results agreeing very closely to within 2%.

— there is not a significant difference in brace force estimate between Models 1-6. Maximum variation is no more than 5% in member 11.

5.2 Effect of joint rigidity on bending moments

Fig. 18 shows the bending moment distribution in the chords and braces for the rigid joint connection case only (Model 1). The critical bending moments of each member obtained with each models are listed in Table 8. Examination of the results reveals the following:

- for chord members, the closer to supports, the larger bending moments they have.
- comparison between Model 1 and 3 shows that there is an increasing of bending moment in the case of semirigid connections.
- comparison between Model 3 and 4 shows that the influence of interaction between two braces in K joint may be increasing bending moments in some members but decreasing in others.
- bending moments induced by axial rigidity in Model 6 greatly exceed that induced by bending rigidity in Model 5.



Note: The bending moment diagrams have been plotted on the side of the member where the stress induced by the bending moment is tensile.

Fig. 18 Bending moment distribution of lattice girder

Table 8 Critical bending moments of CHS lattice girder for different joint models

Member		Critical bending moment (kN-cm)					
		Model 1	Model 2	Model 3	Model 4	Model 5	Model 6
Lower chord	1	4.435	-	7.791	6.882	3.572	8.674
	2	4.567	-	6.264	6.782	4.071	8.002
	3	3.259	-	3.397	4.721	3.250	4.392
Upper chord	8	3.623	-	4.297	5.205	3.435	5.593
	9	5.872	-	9.198	9.434	5.046	11.319
Brace	10	1.938	-	2.685	3.249	1.036	4.630
	11	1.645	-	4.084	2.871	1.149	4.172
	12	1.729	-	3.657	2.615	1.030	4.336

5.3 Effect of joint rigidity on the overall truss deflection

The mid-span truss deflection is given in Table 9 for each of the models considered. From this table it can be found:

— the overall mid-span deflection is very similar for Model 1 (rigid joint model) and Model 2 (pinned joint model).

— weak joint rigidities (Model 3) resulted in increasing the overall deflection by 17.9%, if pinned joint model (Model 2) is taken as a reference. Comparison between Model 3 and 4 reveals that the effect of interaction between two braces in K joint may reduce overall deflection of this girder. Mid-span deflection induced by joint axial rigidity in Model 6 exceeds 33% that induced by joint bending rigidity in Model 5. In Model 6, the semirigid element connecting node k with node i or j in Fig. 14 can be equivalent to a short beam element with axial stiffness calculated as K_N in Eq. (14). But in Model 2, the axial stiffness of this short element is calculated as EA_b/l_e , where A_b is the area of brace section and l_e is the length of the element. If K_N is less than EA_b/l_e , the truss deflection may be underestimated by pin-jointed analysis mainly because of the joint axial flexibility, and vice versa. The girder example in this section just belongs to the former case. The same result has been obtained from the two RHS trusses tested in an experimental program (Frater and Packer 1992).

Table 9 Overall deflection of CHS lattice girder for different joint models

Mid-span deflection (mm)					
Model 1	Model 2	Model 3	Model 4	Model 5	Model 6
-0.066	-0.067	-0.079	-0.096	-0.064	-0.096

5.4 Analysis of secondary stress distribution

According to the conventional definition, secondary stresses are only the bending stresses resulting from truss member continuity at the nodes of a truss with concentric connections.

The primary stress obtained from Model 2, σ_p , and secondary stress obtained from Model 3, σ_s , are summarized in Table 10. Based on this study, several important observations can be made.

Table 10 Primary and secondary stress of CHS lattice girder

Member		Length-to-diameter ratio	σ_p (MPa)	σ_s (MPa)	σ_s/σ_p (%)
Lower chord	1	13.3	0.106	0.104	97.4
	2	13.3	0.266	0.083	31.3
	3	13.3	0.319	0.045	14.2
Upper chord	8	13.3	0.292	0.057	19.6
	9	13.3	0.186	0.122	65.8
Brace	10	19.0	0.455	0.109	23.9
	11	19.0	0.341	0.165	48.5
	12	19.0	0.341	0.148	43.4

— members closer to supports have larger secondary stresses.

— the ratio of secondary stresses to primary ones is significantly affected by the distribution of axial forces. Whether for chords or for braces having larger axial forces, their secondary-to-primary stress ratios are smaller.

— according to EN1993-1-8 (2005), if the length-to-diameter ratios of the members are no less than 6, secondary moments caused by the rotational stiffness of the joints may be neglected. But for this lattice girder, secondary stresses of many members exceed 20% of the primary ones because of axial rigidity of the joints. As a result, the secondary bending moments must be considered in design.

6. Conclusions

An extensive study has been carried out to investigate the rigidity of CHS T, Y and K joints subjected to axial and in-plane bending loads, tubular joints classification, and effect of tubular joint rigidities on the overall response of lattice girders. Based upon the theoretical or numerical results and validation against test results, the following conclusions have been reached:

(1) The brace-to-chord diameter ratio β , and the chord diameter-to-thickness ratio 2γ , have significant effect on the axial and bending rigidity of unstiffened tubular joints, while brace-to-chord thickness ratio τ has marginal influence on them.

(2) Parametric formulae derived from this study can give good predictions for the rigidities of CHS joints.

(3) A classification for tubular joints in Vierendeel lattice girders is proposed in terms of the boundary between rigid and semirigid connections. In this classification, the deformation behavior of lattice girders has been taken into account. This new classification is also applicable to the connections in tubular frame structures.

(4) The numerical example of a Warren lattice girder with different joint models shows some important implications in the practical design of CHS lattice girders:

— the brace and chord member axial forces can be determined with sufficient accuracy on the assumption that the members are pin-connected.

- tubular joint rigidity, particularly axial rigidity will have a significant influence on the bending moments and overall deflections of a steel tubular lattice girder.
- if the joint axial rigidity is less than the axial stiffness of brace within the chord wall, the truss deflection may be underestimated by pin-jointed analysis.

References

- ANSYS (2002), *ANSYS User's Manual Revision 6.1*, ANSYS, Inc., Canonsburg, Pennsylvania.
- Bjorhovde, R., Colson, A. and Brozzetti, J. (1990), "Classification system for beam-column connections", *J. Struct. Eng.*, **116**(11), 3059-3076.
- Choo, Y.S., Liang, J.X., van der Vegte, G.J. and Liew, J.Y.R. (2004), "Static strength of doubler plate reinforced CHS X-joints loaded by in-plane bending", *J. Constructional Steel Research*, **60**, 1725-1744.
- Choo, Y.S., Liang, J.X., van der Vegte, G.J. and Liew, J.Y.R. (2004), "Static strength of collar plate reinforced CHS X-joints loaded by in-plane bending", *J. Constructional Steel Research*, **60**, 1745-1760.
- Chen, Y.Y. and Wang, W. (2003), "Flexural behavior and resistance of uni-planar KK and X tubular joints", *J. Steel & Composite Structures*, **3**(2), 123-140.
- Dexter, E.M., Lee, M.M.K. and Kirkwood, M.G. (1996), "Overlapped K joints in circular hollow sections under axial loading", *J. Offshore Mechanics and Arctic Engineering*, **118**(2), 53-61.
- EN1993-1-1, Eurocode 3: Design of Steel Structures, Part 1-1: General Rules and Rules for Buildings, CEN, 2005.
- EN1993-1-8, Eurocode 3: Design of Steel Structures, Part 1-8: Design of Joints, CEN, 2005.
- Fessler, H. and Mockford, P.B. *et al.* (1986), "Parametric equations for the flexibility matrices of single brace tubular joints in offshore structures", *Proc. Instn Civ. Engrs*, Part 2, **81**, 675-696.
- Frater, G.S. and Packer, J.A. (1992), "Modelling of hollow structural section trusses", *Can. J. Civ. Eng.*, **19**, 947-959.
- France, J.E., Davison, J.B. and Kirby, P.A. (1999), "Strength and rotational stiffness of simple connections to tubular columns using flowdrill connectors", *J. Constructional Steel Research*, **50**, 15-34.
- Furukawa, Y., Makino, Y. and Kurobane, Y. (1998), "Study on out-of-plane rotational stiffness of CHS joints and effective column length of web members in CHS lattice girder", *Tubular Structures VIII*, Singapore, 457-463.
- Gazzola, F. and Lee, M.M.K. (2001), "A numerical investigation into the static strength of CHS K-joints under in-plane moment loading", *Proc. of 9rd Int. Symposium on Tubular Structures*, Düsseldorf, Germany, 175-184.
- Goto, Y. and Miyashita, S. (1998), "Classification system for rigid and semirigid connections", *J. Struct. Eng.*, **124**(7), 750-757.
- Hasan, R., Kishi, N. and Chen, W.F. (1998), "A new nonlinear connection classification system", *J. Constructional Steel Research*, **47**, 119-140.
- Healy, B.E. and Zettlemoyer, N. (1993), "In-plane bending strength of circular tubular joints", *Proc. of 5rd Int. Symposium on Tubular Structures*, Nottingham, U. K., 325-344.
- Healy, B.E. and Zettlemoyer, N. (1994), "Significant issues related to the in-plane bending strength of circular tubular joints", *Proc. of 6rd Int. Symposium on Tubular Structures*, Melbourne, Australia, 191-198.
- Hu, Y.R., Chen, B.Z. and Ma, J.P. (1993), "An equivalent element representing local flexibility of tubular joints in structural analysis of offshore platforms", *Comput. Struct.*, **47**(6), 957-969.
- Hyde, T.H. and Leen, S.B. (1997), "Prediction of elastic-plastic displacement of tubular joints under combined loading using an energy-based approach", *J. Strain Analysis*, **32**(6), 435-453.
- Kurobane, Y. (1998), "Static behavior and earthquake resistant design of welded tubular structures", *Mechanics and Design of Tubular Structures*, Wien, Austria: Springer-Verlag, 53-116.
- Kurobane, Y., Makino, Y. and Ogawa, K. *et al.* (1991), "Capacity of CHS T-joints under combined OPB and axial loads and its interactions with frame behavior", *Proc. of 4rd Int. Symposium on Tubular Structures*, Delft, Netherlands, 412-423.
- Lee, M.M.K. and Dexter, E.M. (1994), "A parametric study on the out-of-plane bending strength of T/Y joints", *Proc. of 6rd Int. Symposium on Tubular Structures*, Melbourne, Australia, 433-440.

- Leen, S.B. and Hyde, T.H. (2000), "On the prediction of elastic-plastic generalized load-displacement responses for tubular joints", *J. Strain Analysis*, **35**(3), 205-219.
- Makino, Y., Kurobane, Y. and Ochi, K. *et al.* (1996), "Database of test and numerical analysis results for unstiffened tubular joints", *IW Doc. XV-E-96-220*.
- Nethercot, D.A., Li, T.Q. and Ahmed, B. (1998), "Unified classification system for beam-to-column connections", *J. Constructional Steel Research*, **45**(1), 39-65.
- Saidani, M. and Coutie, M.G. (1993), "Secondary moments in RHS lattice girders", *Proc. of 5rd Int. Symposium on Tubular Structures*, Nottingham, U. K., 551-559.
- Ure, A. and Grundy, P. *et al.* (1993), "Flexibility coefficients of tubular connections", *Tubular Structures*, London.
- Vegte van der, G.J. (1995), *The Static Strength of Uniplanar and Multiplanar Tubular T and X-joints*, Delft, The Netherlands: Delft University Press.
- Wardenier, J., Kurobane, Y., Packer, J.A., Dutta, D. and Yeomans, N. (1991), *Design Guide for Circular Hollow Section (CHS) Joints under Predominantly Static Loading*, Verlag TÜV Rheinland, Köln.
- Yu, Y. (1997), *The Static Strength of Uniplanar and Multiplanar Connections in Rectangular Hollow Sections*, Delft, The Netherlands: Delft University Press.